Materials Research.
DOI: http://dx.doi.org/10.1590/1980-5373-MR-2017-0997

The Effect of Casting Speed and the Fraction of Al5%Ti1%B Inoculant on the Microstructure and Mechanical Properties of the AA5052 Aluminum Alloy Produced by the Direct Chill Process

***Geraldo Lúcio de Faria*[a]*, *Anderson Santos Leite*[a]**

[a]*Universidade Federal de Ouro Preto, Campus Universitário do Morro do Cruzeiro, Ouro Preto, MG, Brazil*

Received: November 10, 2017; Revised: November 28, 2017; Accepted: December 28, 2017

This study aimed to assess the effect of casting speed and the addition of Al5%Ti1%B inoculant in the casted AA5052 aluminum alloy plate manufactured by the *Direct Chill* process. The focus of this work was to decrease the rejection index of rolled products due to the occurrence of superficial flaws on plates. These defects impact directly on the production costs and on the rolled product quality. The main cause of those flaws is associated with the billet porosity that is related with the excess of atomic hydrogen incorporated into the metallic bath and with the metal shrinkage during solidification. Four different cast conditions were industrially tested, combining two casting speeds and two inoculants amounts. The effect of those variables on the alloy mechanical properties and on their performance in rolling process was also assessed. It was observed that the higher the casting speed and the inoculant fraction, the more refined the microstructure and the lower the fraction and diameter of formed micropores. The increase of casting speed and the inoculant fraction improved the AA5052 alloy rolling performance. The application of these results in an industrial scale performed a decrease from 5.03% to 0.39% per month in the rejection index of rolled products.

Keywords: *AA5052 alloy, casting speed, inoculant Al5%Ti1%B, Direct Chill.*

1. Introduction

The AA5052 alloy is an important product of Al-Mg system applied in the manufacture of components for the transport industry (buses, trucks, ships) and structural components that needs to be lightweight and resistant to corrosion. Usually, these components are formed or machined from AA5052 sheets or bars that are obtained by the rolling of plates. If these semi-products present any volumetric defects during its manufacturing, the next production steps would be adversely affected and the component performance would not meet the specifications.

Nowadays, in South America, the AA5052 alloy is mainly casted by the Direct Chill Process, which is a semi-continuous vertical casting device. Some studies about the Direct Chill process showed that, the melt temperature and casting speed have a great influence on solid macrossegregation and on billet porosity[1-3].

The porosity of the obtained solid-state metal has a strong influence on subsequent forming process, especially on aluminum alloy rolling. Depending on the pore characteristics, during the plate rolling, flaws as superficial bubbles (hot rolling) and scales (cold rolling) may occur (Figure 1). Nowadays, for the AA5052 aluminum alloy, this problem affects 5.03% of the rolled products in South America, causing a high financial setback and internal operational problems due to the generation of scrap.

Piwonka[4] affirmed in a review paper that parameters as casting speed and alloy grain refiner have strong influence on porosity formation during Al alloy solidification. This important review work highlights the importance of establishing correct process parameters to obtain a high quality plate. Aiming to better understand the porosity formation in Al alloy casting process, Lee[5] proposed a mathematical model to correlate the microporosity to the hydrogen segregation and metal shrinkage during solidification. They showed that during the metal solidification, the atomic hydrogen rejected by the solid front, where it has low solubility, enriches the liquid phase continually. When the liquid reaches critical levels of hydrogen in the solution, molecular hydrogen bubbles start to form.

*e-mail: geraldolfaria@yahoo.com.br

Funding: This research did not receive any specific grant from funding agencies in the public, commercial, or not-for-profit sectors.

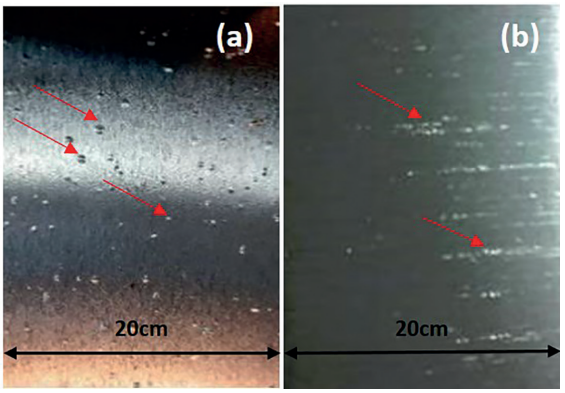

Figure 1. a) Bubble-type flaw on a hot rolled AA5052 alloy (final sheet thickness: 9.52mm), b) scale-type flaw on a cold rolled AA5052 alloy (final sheet thickness: 3.20mm)

The technical literature affirms that the occurrence of this phenomenon depends on several parameters: the alloy chemical composition and its contraction characteristics during solidification, the solidification speed, the temperature gradient and the initial hydrogen fraction in the bath. They also affirm that the porosity of the solid-state metal occurs due to the liquid incapacity to fill the bubbles during the metal continuous cooling and solidification (the volume shrinkage associated with solidification cannot be compensated by the interdendritic flowing opposite to the displacement of the isotherms). All those variables affect the amount, size and morphology of formed pores[1-7].

Gali[7], as well, Weiler and Wood[8] studied the development of micro-crakcs in Al-Mg and Mg alloys during hot rolling. The authors showed that cracks on the alloy surface were initiated mainly at pores and grain boundaries attributable to the stress concentration and grain boundary sliding mechanism. In this context, they reinforced the importance to better understand the relations between casting process parameters to obtain high quality plates and to guarantee the performance of rolled products.

The technical literature presents that the casting speed for the Direct Chill process is an important operational parameter, because it has a direct influence on three variables: the metal solidification temperature, solidification speed and its temperature distribution. Small changes in casting speed affect the Direct Chill thermal profile, modifying the position of isothermal lines, affecting the resulting microstructure and microporosity[9-14].

The grain refiner tool is mentioned as an important technological resource to obtain a homogeneous and refined microstructure in casted plates. It consists to obtain fine and axial grains through the controlled addition of inoculants in the liquid metal, favoring the heterogeneous nucleation mechanism[15-19]. According to Easton and Stjohn[14], the type of inoculant often used for aluminum alloys are based on the addition of Al, Ti and B.

In this context, this work studied the effects of the casting speed and the inoculant Al5%Ti1%B addition on microstructure, mechanical properties and rolling performance of the AA5052 aluminum alloy produced by Direct Chill method. It was not found in technical literature any work about the effects of Direct Chill processing variables on the occurrence of rolling flaws in the AA5052 alloy, aiming to decrease them. This paper presents an important contribution, proposing a potential solution to decrease the rolling rejection index through the casting process adjustment.

2. Materials and Methods

Samples of the AA5052 alloy were manufactured by the mix of a chemical controlled scrap and liquid metal obtained by the Bayer process. The obtained liquid metal was transferred to the casting furnace, where it was scarified aiming to remove alkali elements, such as Na, Ca and Li. In a minor proportion, chlorines were added to decrease the hydrogen concentration. At the same stage, the argon gas was inserted to movement the bath and draw out formed hydrogen molecules. The Figure 2-a presents a basic flowchart of the manufacturing process used in this work (typical process in South America industrial facilities).

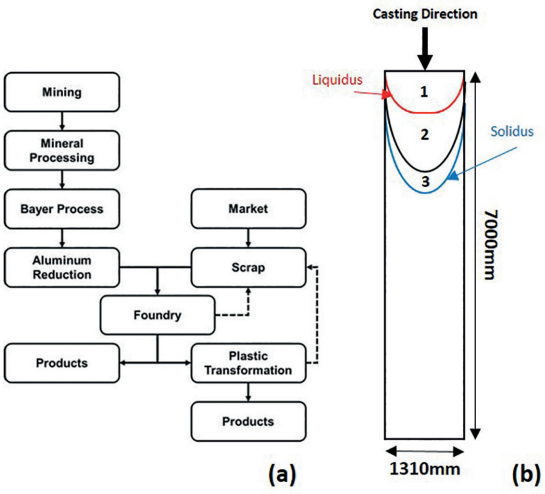

Figure 2. a) Schematic representation of the manufacturing route to obtain the samples of AA5052 aluminum alloy, b) Schematic representation of the liquidus (L) and solidus (S) isothermal transition zone in a casting crucible. The isothermal coherency is defined as 30%. (1) The liquid reservoir depth; (2) transition zone; (3) mushy zone

After the check of the alloy chemical composition, the liquid metal was casted in a Direct Chill system. This procedure was performed 48 times, for each one, some casting parameters were held constant (Table 1). The evaluated parameters were the final casting speed (S_F) (70 and 80mm/min.) and

Table 1. Casting parameters that were held constant during plates manufacturing.

Casting Temperature (T_c)	Initial Casting Speed (S_I)	Initial Inoculant Addition Speed (V_{IA})	Initial Water Flow (Q_I)	Inlet Water Temperature (T_I)	Outlet Water Temperature (T_O)	$MgNa_2Cl_4$Addition (Q_F)
720ºC	50mm/min.	2300mm/min.	250m^3/h	(24 ± 2)ºC	(32 ± 2)ºC	20kg

the inoculant amount (4 and 7kg/ton.). Table 2 summarizes four different casting conditions that were evaluated. For each one, 12 plates were manufactured in an industrial scale making this study strongly representative. It is important to emphasize that the current condition usually applied in South America industries is the A1 (Table 2).

Table 2. Process parameters assessed in this study: final casting speed and inoculant addition.

Process Parameters	Casting Speed (S_F) [mm/min.]	Inoculant addition [kg/ton.]	Number of produced plates
A1	70	3.94	12
A2	70	7.88	12
B1	80	3.45	12
B2	80	6.90	12

The alternative final casting speed (80mm/min.) and the selected inoculant amount (7kg/ton.) were chosen focusing not only to refine the plate microstructure, but also to prevent other operational problems as billet warping, that could occur with higher casting speeds; the change of the alloy chemical composition due to the use of higher inoculant amount, avoiding the requested chemical specifications were meet.

Figure 2-b is a schematic figure that illustrates the isothermal lines during the alloy solidification in a Direct Chill process. It is also possible to observe the size of the used crucible and the solidification direction. The produced plates had the following dimensions: 1310mm wide, 240mm thick and 7000mm long (Figure 3-a). According to Liu and Morris[17], the expected microstructure for this type of alloy is composed mainly by α phase, with intergranular β precipitate (Al_xMg_y).

The manufactured plates of AA5052 alloy were characterized as casted. Slices were collected perpendicularly to the casting direction at the plate center (Figure 3-a). From these slices, 240mm long samples were removed at the left side edge (Figure 3-b). The mechanical tests and metallographic specimens were machined as showed in Figure 3-c.

The produced samples were chemical analyzed in an optical emission spectrometer ARL. The microstructural characterization was performed by Polarized Light Optical microscope (OM). Aiming to reveal the microstructures, metallographic procedures were applied: mechanical grinding and polishing, followed by anodizing using an aqueous solution of 1.8wt.% fluo boric acid (HBF_4). Quantitative metallographic procedures were applied aiming to determine pore diameters, pore amount and the α phase grain size. For each characterized sample, the number of quantified fields were determined in accordance with the need to meet 95% of confidence (ASTM E112-13).

In order to carry out the tensile tests, five specimens were machined for each casting condition. They were prepared according to the ASTM E8/E8M[18] standard (Length of reduction section=57mm; Gage length=50mm; Width=12.5mm, Thickness=4.0mm). The tensile tests were performed in a EMIC DL5000/700 machine. The tested specimens were fractographically analyzed using a VEGA 3 SEM. The Brinell hardness tests were carried out based on the ASTM E10[19] standard in a VebWerkstoffprüf machine. The average hardness values were calculated from five measurements.

Besides the laboratorial tests, statistical data analyses were performed aiming to examine the influence of studied operational parameters on microstructural characteristics, mainly on the microporosity. The Contour Graph method was applied using the software Minitab17. This method uses a contour plot to explore the potential relationship between three variables. Contour plots display the 3-dimensional relationship in two dimensions, with x- and y-factors (predictors) plotted on the x- and y-scales and response values represented by contours. A contour plot is like a topographical map in which x-, y-, and z-values are plotted instead of longitude, latitude, and elevation. In this study, the predictors were the studied parameters (casting speed and inoculant amount) and the response, or the method output was their influence on microstructural parameters (shell zone, α grain size, pore diameter and pore amount).

In accordance with the obtained results, the condition that promoted the most favorable plate characteristics was applied in an industrial scale for six months. The casted plates were hot and cold rolled and the rejection indexes due to flaws occurrence were monthly calculated.

3. Results and Discussion

3.1 Chemical analysis

Table 3 presents the chemical compositions of the AA5052 plates manufactured with the proposed combinations of casting speed and inoculant addition. It is possible to observe that all obtained chemical compositions meet the ASTM B209[20] standard requirements for the commercial AA5052 alloy. The

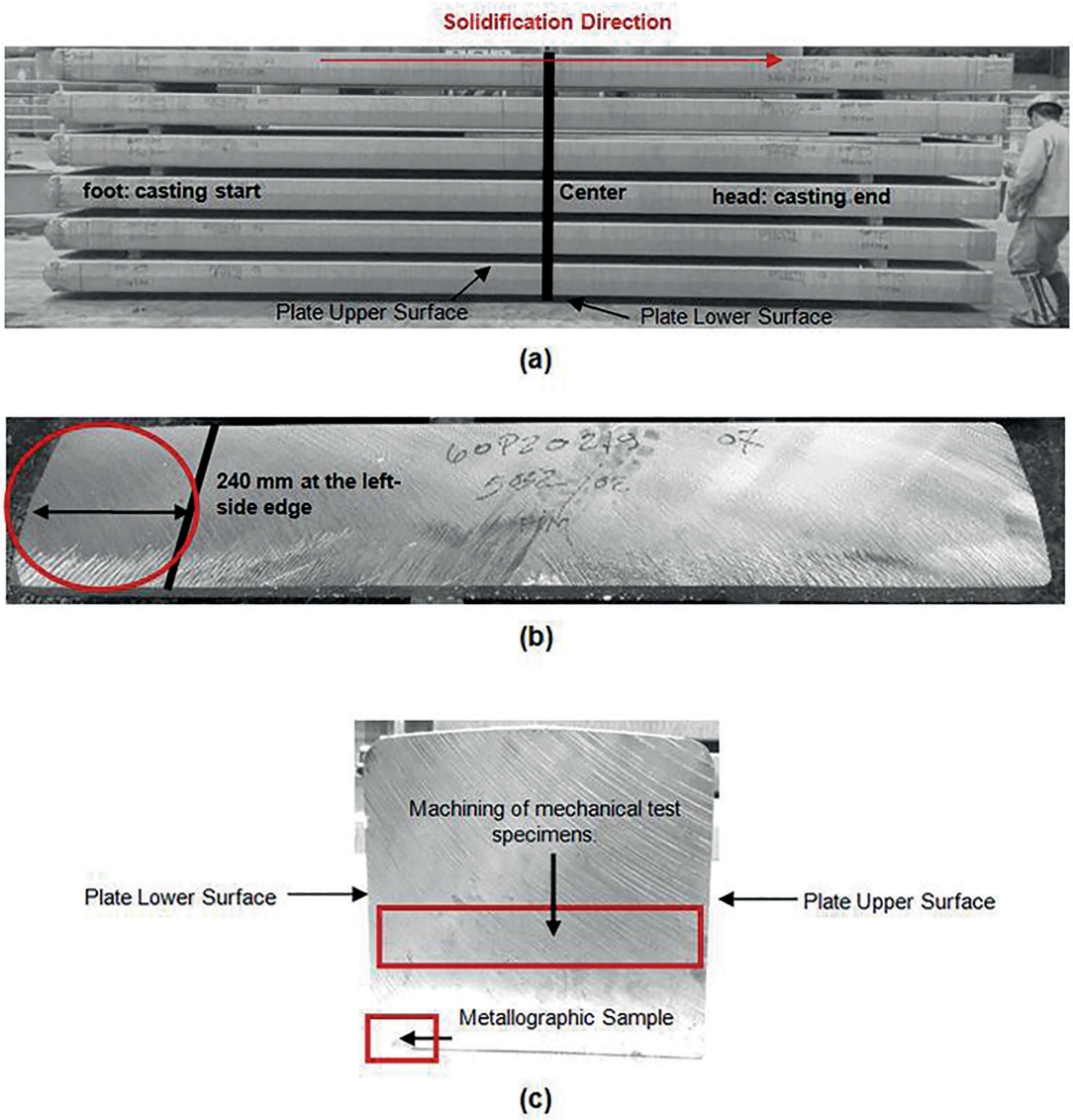

Figure 3. a) Casted plates, where it is possible to observe the central area from where the slices were collected, b) Transversal slice from where samples were collected, c) Sampling areas for microstructural analysis, hardness and tensile tests

proposed inoculant addition has not influenced significantly the alloy chemical requirements. It is important to highlight that the Ti and B contents are not specified in AA5052 chemical requirements. These elements are considered as "others" and they are limited to 0.15wt.%, value that was not reached, even with the increase of inoculant addition.

Table 3. Chemical composition of studied plates (wt.%).

Sample		Al	Mg	Fe	Cr	Si	Cu	Mn	Zn	Others
ASTM	Max.	97.70	2.80	0.40	0.35	0.25	0.10	0.10	0.10	0.15
	Min.	95.70	2.20	-	0.15	-	-	-	-	-
A1		96.97	2.30	0.29	0.19	0.11	0.014	0.04	-	0.09
A2		96.94	2.40	0.31	0.16	0.12	0.020	0.03	-	0.02
B1		96.89	2.30	0.34	0.18	0.13	0.009	0.04	-	0.11
B2		97.10	2.20	0.28	0.19	0.10	0.014	0.04	-	0.08

3.2 Microstructural characterization

Figure 4 presents the microstructures of samples A1, A2, B1 and B2. In all of them, it is possible to observe α-Al-Mg solid solution (white surface) and β (Al_xMg_y) intergranular precipitates (pointed with red arrows), in accordance with Liu and Morris[17]. It is also possible to verify sample microporosities (size and morphology). It was verified that the higher the casting speed and the higher the inoculant addition, more homogenous and refined the microstructure, with more disperse and smaller β precipitates and minor pore average sizes (metallographically quantified and presented in Figure 5). The sample B2, which was manufactured with the highest casting speed and the largest amount of inoculant, presented the best-obtained microstructure.

Figure 6 shows the polarized light micrographs of manufactured samples. It is possible to observe a significant change on α average grain sizes (ATSM E 112-13 Standard[21]) and on micropore size and distribution. Table 4 presents the α phase average grain sizes and Figure 5 highlights the main characteristics of micropores in function of the manufacturing condition (95% of confidence, respecting the mentioned standard requirements).

It is important to notice that the inoculant addition and the increase of the casting speed had a strong influence on the structure grain size. The higher the inoculant addition and the higher the casting speed, the smaller the grain size.

The increase of the inoculant amount promoted a significant increase of the preferential sites for α grain nucleation (heterogeneous nucleation), increasing its nucleation rate. The increase of the casting speed increased the liquid super-cooling, decreased the critical radius of solid nuclei and restricted its growth. These combined factors contributed to the decrease of the final average grain size. It was noticed that the minor grain size was obtained for B2 sample, which was manufactured with the highest combination of inoculants addition and casting speed. Weiler and Wood[8] affirmed that the grain refinement can promote the decrease of plate residual stress, the increase of mechanical strength and the improvement of rolled surface finishing.

Evaluating the microporosity and the extension of the shell zone (heterogeneous portion solidified in contact with the mold interface), it was verified that both parameters followed the same tendency of the grain size profile (Figure 5). The smaller the grain size, the lower the micropore amount and the shorter the shell zone extension. The B2 sample presented

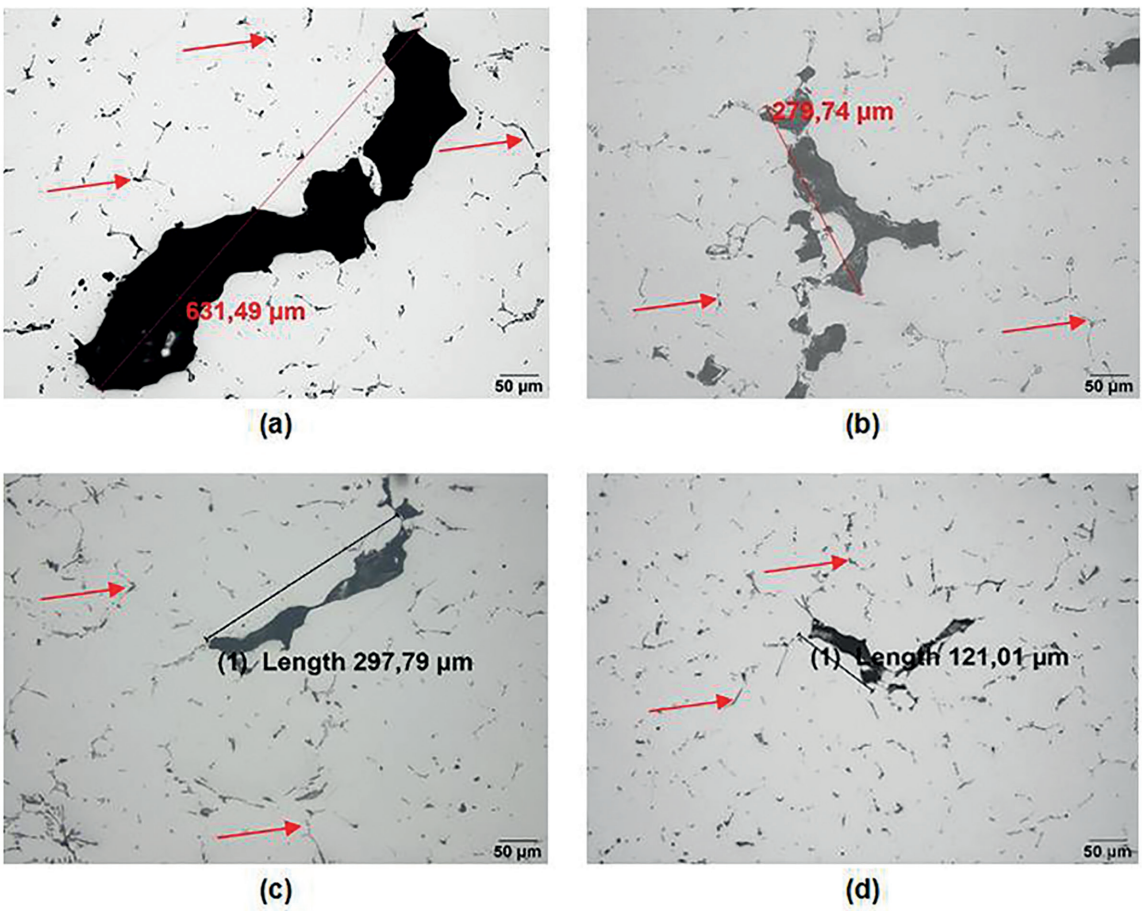

Figure 4. Microstructures of samples a) A1, b) A2, c) B1, d) B2 (β precipitates are pointed with red arrows)

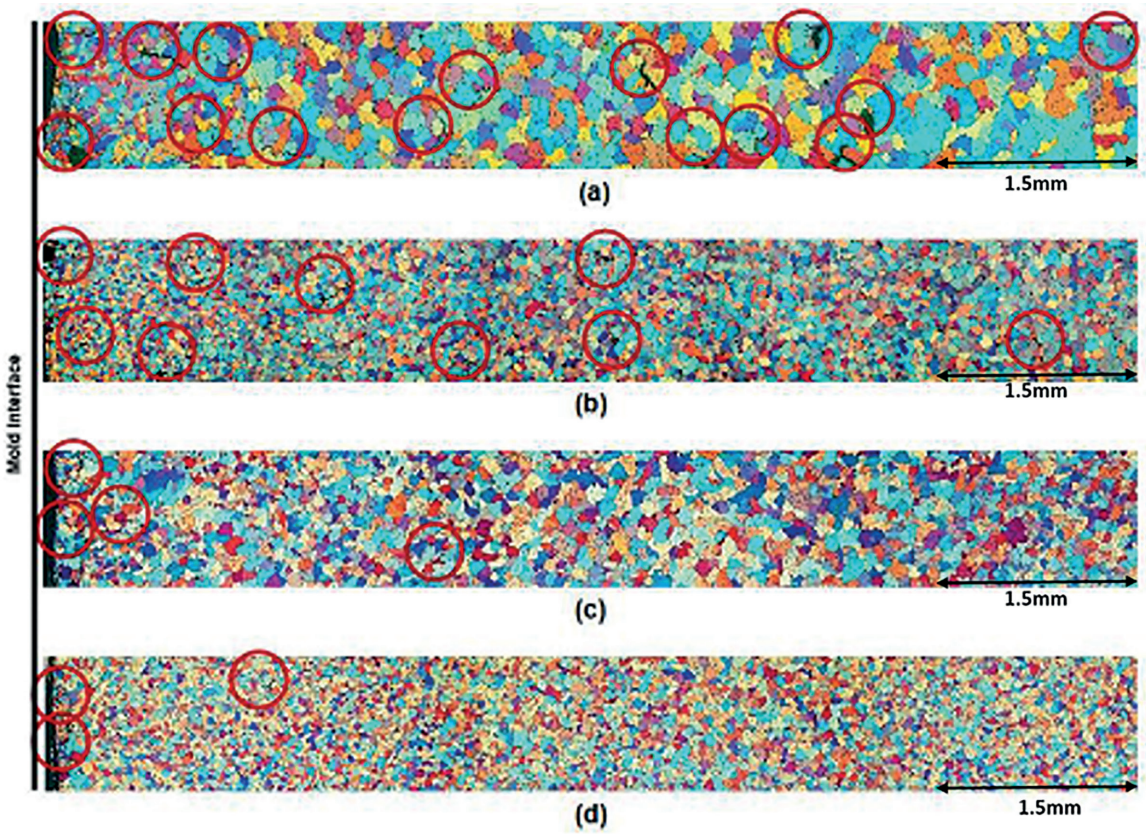

Figure 5. a) Pore diameters versus pore amount, b) Pore diameters versus α average grain size, c) Pore amount versus *shell zone*, d) Pore amount versus α average grain size (95% of confidence)

the best structural condition with the lowest values of grain size, micropore fraction and shell zone extension.

The decrease of the shell zone with the casting speed increase was due to changes in the heat transfer profile. These results are in accordance with previous studies about Direct Chill process done by Eskin[3] and Hao[9].

Liu[10] showed that the most part of microporosity in aluminum alloys is resulted from the incomplete feeding in the mushy zone. The volume shrinkage associated with solidification cannot be compensated by the interdendritic flowing opposite to the displacement of the isotherms. While the temperature decreases during solidification, the solubility of hydrogen decreases quickly, but the real concentration of the element in the liquid increases due to its segregation. The increase of cooling rate promotes a higher metal volumetric contraction and consequently the increase of internal pressure of dissolved hydrogen. This may form retraction voids and decreases de hydrostatic pressure for precipitation of molecular hydrogen, creating favorable conditions for micropore formation.

The A1 condition, which corresponds to the current process condition, presented the worst structural characteristics. This is, probably, due to the occurrence of a shorter liquid zone (above the liquidus line in Figure 2-b) which accelerates the solidification process in relation to B1 and B2 conditions, intensifying the hydrogen atoms imprisonment.

Comparing A1 and A2 samples in Figures 5-a and 5-b, it is possible to observe that for the same casting speed, the increase of inoculant amount decreased the microporosity, but slightly increased the pore diameters. It is supposed that the finer the structure, the higher the grain boundary density. As the grain boundary works as a preferential hydrogen diffusion way from solid to liquid phase, for smaller grain sizes (higher solid nucleation rate) the hydrogen imprisonment decreases at liquid-solid interface, decreasing the microporosity.

However, the pore diameter slightly increased because the inoculant addition increased the solid nucleation rate and the local hydrogen segregation increased in some specific points. As the solidification speed was not changed, there was enough time to form bigger bubbles that justifies the increase of pore size. When the casting speed was increased to 80mm/min., even with the highest inoculant amount (B2 condition), a larger liquid zone was obtained, changing the DC heat profile and increasing the feed material availability in solidification front, decreasing significantly the metal shrinkage effect. This effect possibly was more effective than the increase of the inoculant amount and consequently decreased the pore diameters. Those effects are in accordance with previous works[10,12,22].

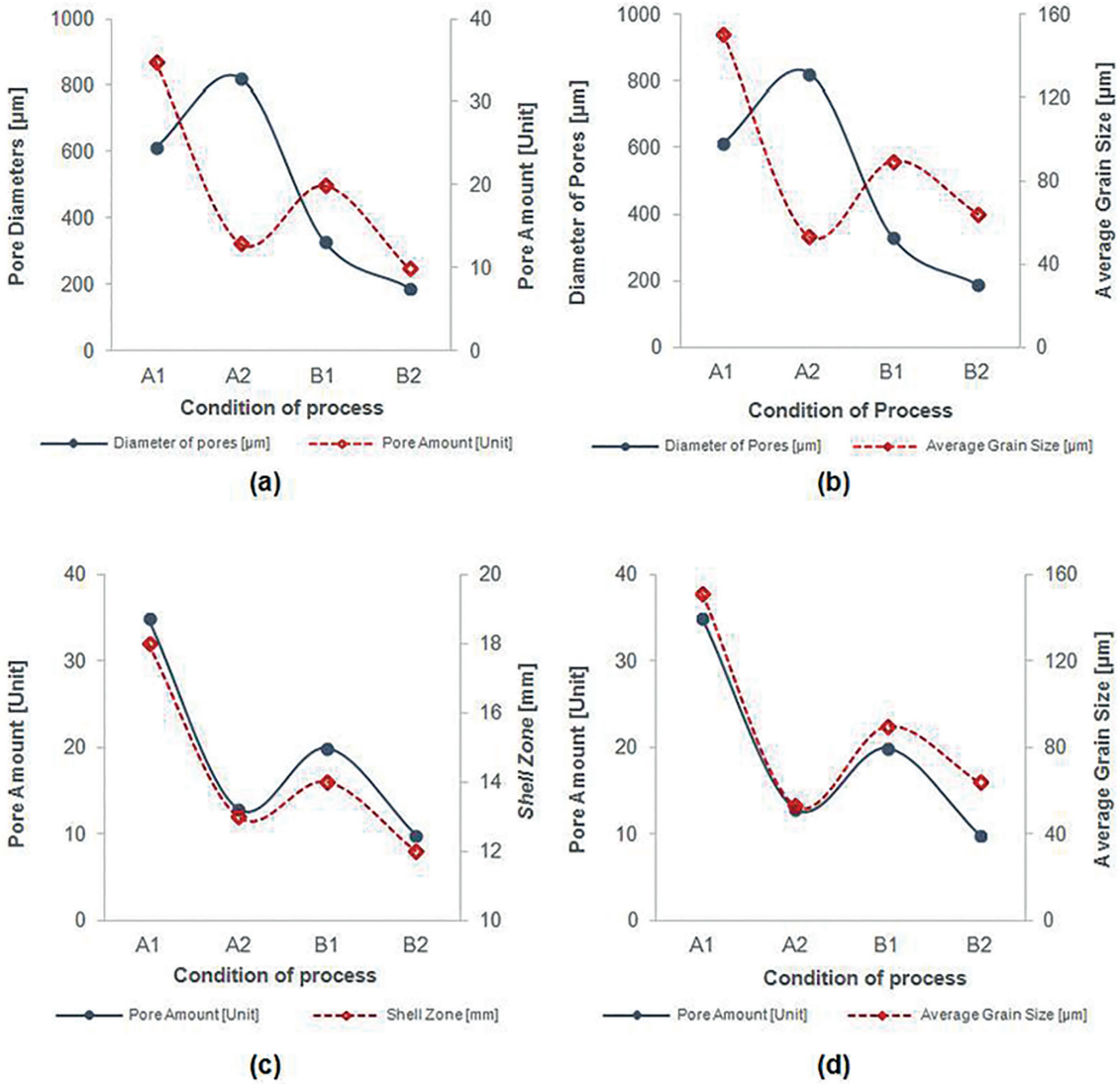

Figure 6. Polarized light micrographs a) A1,b) A2,c)B1, d) B2

Table 4. Average grain sizes of α phase (95% of confidence).

Process Parameter	Grain Number ASTM E 112	ϕ (Grain diameter) [µm]
A1	2.5	151
A2	5.5	53
B1	4	90
B2	5	64

3.3 Statistical analysis for the direct chill process

A descriptive statistical analysis with a 95% confidence interval was carried out aiming to evaluate the specific influence of casting speed and inoculant amount on: *shell zone* depth (mm), pore diameter (µm); pore amount (unit); α average grain size (µm). Figure 7 presents statistical contour maps that show: 1) the combined effects of casting speed increase and inoculant addition may strongly decrease de shell zone depth and decrease the plate microporosity; 2) the inoculant addition is more effective on α grain size than the casting speed; 3) The casting speed is more effective on pore diameters than the inoculant addition.

3.4 Mechanical tests

Table 5 presents the Brinell hardness results obtained for the AA5052 samples. An increase of 3.8% in the hardness values was observed for the A2 and B2 conditions compared to A1 and B1. It is well known that the grain refinement is an important hardening mechanism used to increase the material mechanical strength and its toughness. As already discussed, the A2 and B2 conditions presented the lowest grain sizes, because the inoculant amount had stronger effect than casting speed on α grain size (highlighted in Figures 6 and 7-b), explaining this slightly hardness increase.

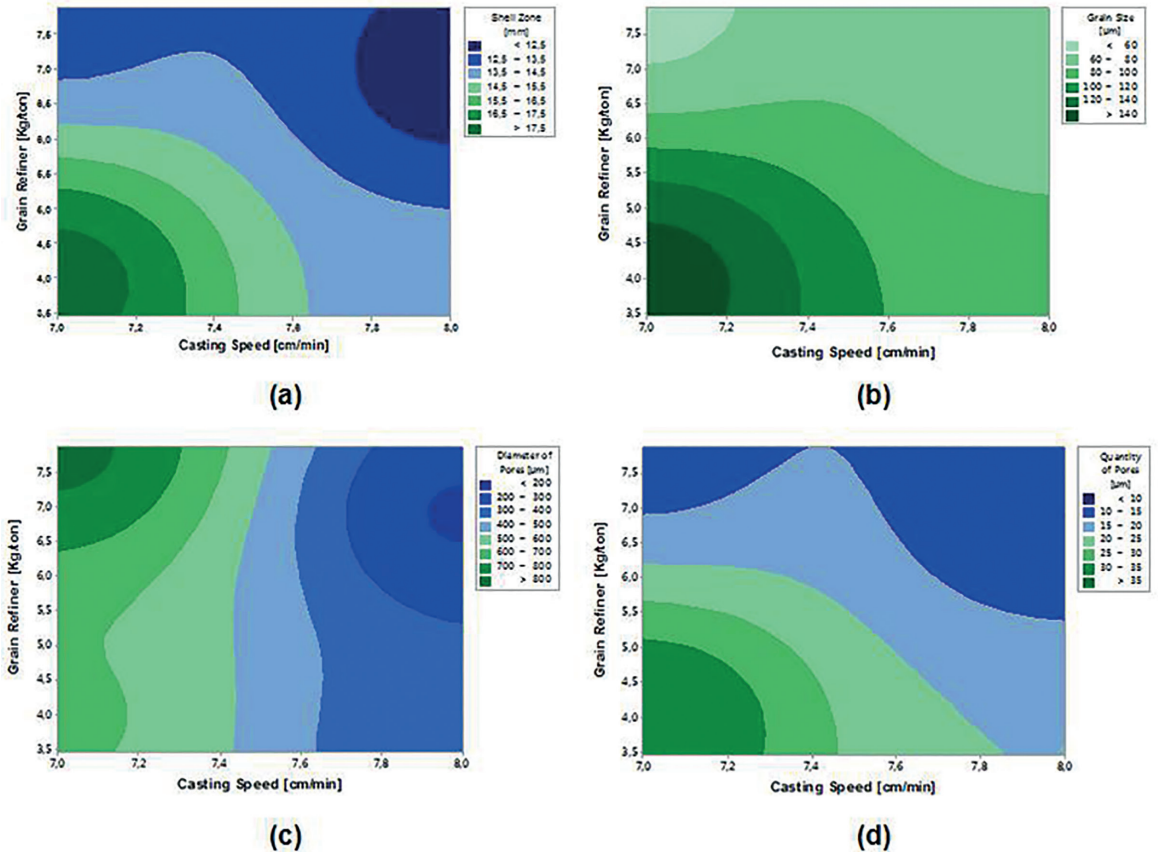

Figure 7. Statistical analysis of the independent variable effects on studied structural parameters

Table 5. Brinell hardness results.

	A1	A2	B1	B2
Average	53	55	53	55
Standard Deviation	1.0	1.0	0	0
Confidence Index (95%)	1.4	0.9	0	0

Table 6 presents the tensile test results and Figure 8 presents fractographs of tested specimens produced according to A1 and B2 conditions. It was noticed that, considering the experiment standard deviations, no significant variations occurred on measured properties and the specimen behaviors were ductile (predominance of dimples). Probably, this occurred due to a balance of effects: while the α grain refinement contributed to increase the material mechanical strength and ductility, the increase of β precipitation at α grain boundaries contributed to decrease those properties.

This is an important result, because the maintenance of yield and ultimate tensile, as well as the elongation, in relation to A1 condition (condition used nowadays in rolling plans) guarantees that: it is not necessary to increase the rolling loading; the material plasticity will be enough to allow its successful processing. Considering the low pore amount of A2 and B2 conditions, it was supposed that for the same rolling conditions the occurrence of superficial flaws, especially for B2 condition, would strongly decrease.

Aiming to validate this supposition, during six months, all produced plates were industrially manufactured applying the B2 condition (casting speed of 80mm/min. and inoculant addition of 6.90kg/ton.) and monitored from the foundry until to the rolling. The obtained results are presented in the next topic.

3.5 Operational analysis of plate rolling

Figure 9 presents a comparative study about the rejection index of AA5052 rolled products during a year (sequence of hot and cold rolling). From January until June, the plates were manufactured according to the A1 condition. From June until December, they were produced according to B2 new proposed condition. It is noticeable a significant decrease of the rejection index (rejection due to the occurrence of superficial flaws classified as bubbles or scales) from an average value of 5.03% to 0.39%. These results confirmed the expectations generated in the bench scale characterization.

Figure 10 presents the superficial aspect of manufactured rolled plates according to the B2 condition. It was possible to observe surfaces free from flaws and approved according to a visual quality control. Besides this, other advantages have been achieved: decrease of operational costs; increase of the Direct Chill system productivity holding the foundry quality and improving the surface quality of rolled products.

Table 6. Tensile test results (YS – yield strength, UT – ultimate tensile, ε - elongation).

	YS [MPa]				UT [MPa]				ε [%]			
	A1	A2	B1	B2	A1	A2	B1	B2	A1	A2	B1	B2
Average	83	80	78	79	177	177	171	177	26	26	23	24
Standard Deviation	3.0	1.0	2.0	4.0	1.0	1.0	1.0	1.0	0.4	0.7	2.0	2.0
Confidence Index [95%]	4.1	1.7	2.4	4.3	1.4	1.6	1.4	0.8	0.5	0.9	2.0	1.8

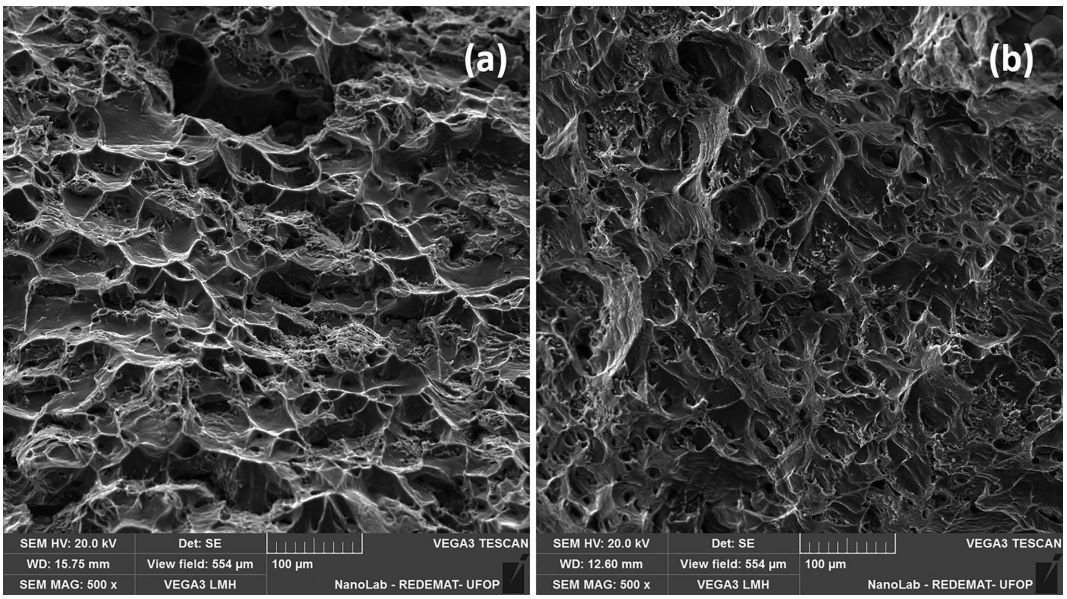

Figure 8. SEM fractographs of tested specimens (a) A1 condition (reference), (b) B2 condition (new proposition)

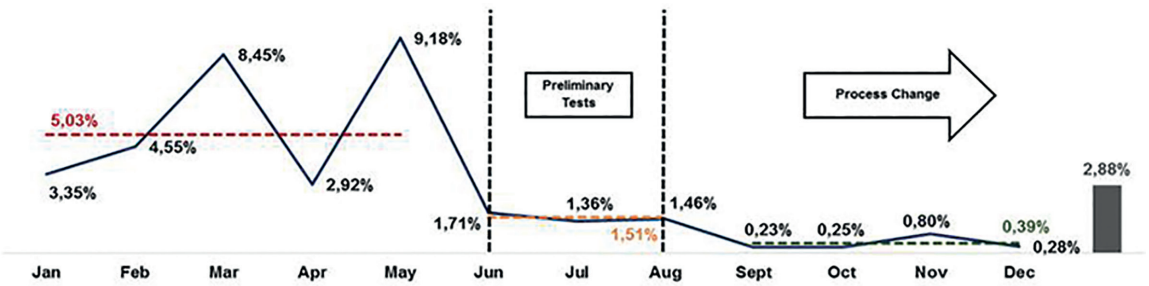

Figure 9. Comparative data of industrial rejection indexes measured for plates manufactured according to A1 condition (Jan-Jun) and according to the new proposed B2 condition (Jun-Dec)

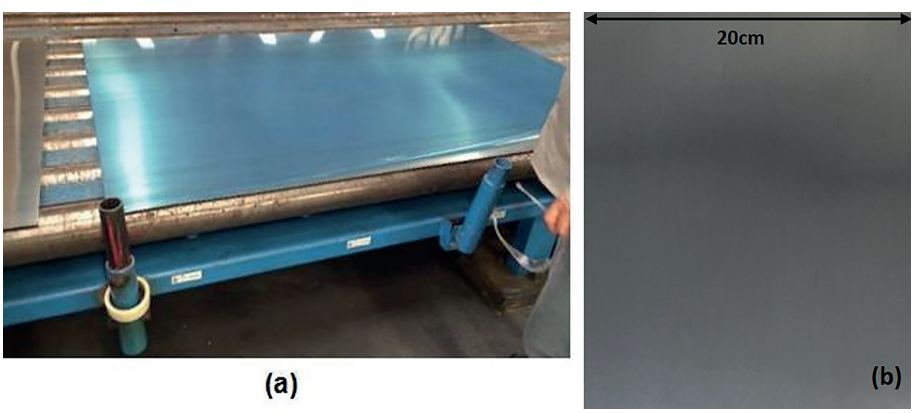

Figure 10. a) Picture of rolled AA5052 sheet highlighting the surface quality after the employ of proposed B2 foundry condition (1200mmx2000mmx0.80mm sheets), b) detail of a rolled sheet surface without flaws

It is important to highlight that all plates produced during the evaluated year were destined to different applications. Due to that, they were submitted to different hot and cold rolling plans, with different final thickness and with different mechanical requirements. All rolled products approved due to the absence of superficial flaws, also met the mechanical specifications required for their applications.

4. Conclusions

In the AA5052 aluminum alloy manufacturing process, the increase of Al5%Ti1%B concentration as inoculant (from around 3.5kg/ton. to 7kg/ton.) allowed that the produced alloys meet the chemical specifications recommended by ASTMB209 standard.

The increase of casting speed from 70mm/min. to 80mm/min., combined with the increase of inoculant amount, allowed to obtain a more refined microstructure with lower fraction and smaller pores, and a shorter shell zone extension in plates solidified by the *Direct Chill* process.

For the assessed conditions, the addition of a higher concentration of inoculants had a more significant effect on the decrease of alloy grain size in comparison with the increase of casting speed. However, the increase of cooling rate proved to be an important parameter related with the pore amount decrease. The increase of casting speed had also an important effect on the decrease of the process input consumption and on the facility productivity.

Despite the important effects of the proposed changes herein for grain refinement and porosity decrease, suggesting a minor hydrogen imprisonment in the solid phase and solidification conditions, there was no significant variation on the mechanical properties of solidified plates. This result ensures the non-need to change the usual rolling route and it guarantees the plate good performance during the subsequent mechanical forming.

Operational studies, carried out in an industrial facility for twelve months, showed that the proposed changes on Direct Chill casting process for AA5052 alloy were efficient regarding the initial objectives. For the processing condition with the highest casting speed and highest inoculant addition, it was possible to achieve the lowest rejection index (average value of 0.39%per month) due to the occurrence of superficial flaws during the rolling process.

5. Acknowledgements

The authors thank the CBA Company for kindly providing materials for this study and for making the industrial tests possible.

6. References

1. Nadella R, Eskin DG, Du Q, Katgerman L. Macrosegregation in direct-chill casting of aluminium alloys. *Progress in Materials Science*. 2008;53(3):421-480.

2. Suyitno, Savran VI, Katgerman L, Eskin DG. Effects of alloy composition and casting speed on structure formation and hot tearing during direct-chill casting of Al-Cu alloys. *Metallurgical and Materials Transactions A*. 2004;35(11):3551-3561.

3. Eskin DG, Savran VI, Katgerman L. Effects of melt temperature and casting speed on the structure and defect formation during direct-chill casting of an Al-Cu alloy. *Metallurgical and Materials Transactions A*. 2005;36(7):1965-1976.

4. Piwonka TS, Kuyucak S, Davies KG. Shrinkage-related porosity in steel castings: a state-of-the-art review. *AFS Transactions*. 2002;110(2):1257-1270.

5. Lee PD, Hunt JD. Hydrogen porosity in directionally solidified aluminum-copper alloys: a mathematical model. *Acta Materialia*. 2001;49(8):1383-1398.

6. Jahangiri A, Marashi SPH, Mohammadaliha M, Ashofte V. The effect of pressure and pouring temperature on the porosity, microstructure, hardness and yield stress of AA2024 aluminum alloy during the squeeze casting process. *Journal of Materials Processing Technology*. 2017;245:1-6.

7. Gali OA, Shafiei M, Hunter JA, Riahi AR. A study of the development of micro-cracks in surface/near surface of aluminum-manganese alloys during hot rolling. *Materials Science and Engineering: A*. 2015;627:191-204.

8. Weiler JP, Wood JT. Modeling fracture properties in a die-cast AM60B magnesium alloy II- The effects of the size and location of porosity determined using finite element simulations. *Materials Science and Engineering: A*. 2009;527(1-2):32-37.

9. Hao H, Maijer DM, Wells MA, Cockcroft SL, Sediako D, Hibbins S. Development and validation of a thermal model of the direct chill casting of AZ31 magnesium billets. *Metallurgical and Materials Transactions*. 2004;35(12):3843-3854.

10. Liu Y, Jie W, Gao Z, Zheng Y. Investigation on the formation of microporosity in aluminum alloys. *Journal of Alloys and Compounds*. 2015;629:221-229.

11. Spinelli JE, Ferreira IL, Garcia A. Influence of melt convection on the columnar to equiaxed transition and microstructure of downward unsteady-state directionally solidified Sn-Pb alloys. *Journal of Alloys and Compounds*. 2004;384(1-2):217-226.

12. Lee PD, Atwood RC, Dashwood RJ, Nagaumi H. Modeling of porosity formation in direct chill cast aluminum-magnesium alloys. *Materials Science and Engineering: A*. 2002;328(1-2):213-222.

13. Quested TE, Greer AL. Grain refinement of Al alloys: Mechanisms determining as-cast grain size in directional solidification. *Acta Materialia*. 2005;53(17):4643-4653.

14. Easton M, StJohn D. Grain refinement of aluminum alloys: Part I. The nucleant and solute para-digms - a review of the literature. *Metallurgical and Materials Transactions A*. 1999;30(6):1613-1623.

15. Birol Y. Grain refinement and modification of Al-Si foundry alloys with B and Sr additions. *Materials Science and Technology*. 2014;30(10):1154-1161.

16. Qiu D, Taylor JA, Zhang MX, Kelly PM. A mechanism for the poisoning effect of silicon on the grain refinement of Al-Si alloys. *Acta Materialia*. 2007;55(4)1447-1456.

17. Liu JT, Morris JG. Recrystallization microstructures and textures in AA5052 continuous cast and direct chill cast aluminum alloy. *Materials Science and Engineering: A*. 2004;385(1-2):342-351.

18. ASTM International. *ASTM E8/E8M-16a - Standard Test Methods for Tension Testing of Metallic Materials*. West Conshohocken: ASTM International; 2016.

19. ASTM International. *ASTM E10-17 - Standard Test Method for Brinell Hardness of Metallic Materials*. West Conshohocken: ASTM International; 2017.

20. ASTM International. *ASTM B209-14 - Standard Specification for Aluminum and Aluminum-Alloy Sheet and Plate*. West Conshohocken: ASTM International; 2014.

21. ASTM International. *ASTM E112-13 - Standard Test Methods for Determining Average Grain Size*. West Conshohocken: ASTM International; 2013.

22. Lee PD, Chirazi A, Atwood RC, Wang W. Multiscale modelling of solidification microstructures including microsegregation and microporosity, in an Al-Si-Cu alloy. *Materials Science and Engineering A*. 2004;365(1-2):57-65.